

## Article

# Permeable Pavements for Flood Control in Australia: Spatial Analysis of Pavement Design Considering Rainfall and Soil Data

Asif Iqbal <sup>\*</sup>, Md Mizanur Rahman  and Simon Beecham 

UniSA STEM, University of South Australia, Mawson Lakes, SA 5095, Australia;  
mizanur.rahman@unisa.edu.au (M.M.R.); simon.beecham@unisa.edu.au (S.B.)

\* Correspondence: asif.iqbal@unisa.edu.au

**Abstract:** Permeable pavements allow rainfall and surface runoff to infiltrate through their surface, and this reduces urban flooding by increasing water management efficiency. The design of permeable pavements depends heavily on rainfall and soil conditions for a particular area. This study investigates the required base course thickness in different areas across Australia that can effectively reduce flood intensities. A detailed hydraulic analysis was conducted, considering the pavement materials, soil characteristics and rainfall intensities across Australia. The research also developed a relationship between base course thickness, rainfall intensity and soil classification, which can facilitate reasonable predictions of required design thickness for any location. The results showed a strong relationship between soil characteristics and pavement thickness, with clay soils requiring increased pavement thickness correlated with rainfall intensity. A spatial analysis was conducted, producing a tool for initial screening on the design requirements, before proceeding with a detailed design.



**Citation:** Iqbal, A.; Rahman, M.M.; Beecham, S. Permeable Pavements for Flood Control in Australia: Spatial Analysis of Pavement Design Considering Rainfall and Soil Data. *Sustainability* **2022**, *14*, 4970. <https://doi.org/10.3390/su14094970>

Academic Editor: Edoardo Bocci

Received: 28 March 2022

Accepted: 20 April 2022

Published: 21 April 2022

**Publisher's Note:** MDPI stays neutral with regard to jurisdictional claims in published maps and institutional affiliations.



**Copyright:** © 2022 by the authors. Licensee MDPI, Basel, Switzerland. This article is an open access article distributed under the terms and conditions of the Creative Commons Attribution (CC BY) license (<https://creativecommons.org/licenses/by/4.0/>).

**Keywords:** permeable pavements; flood control; pavement design; spatial analysis

## 1. Introduction

Natural disasters are a major concern for Australia that cost approximately AUD 9 billion in 2015, and are anticipated to increase to AUD 33 billion by the year 2050 [1]. Flooding is a prominent disaster in Australia, costing about 29% of the total disaster costs due to damage to the built environment and subsequent loss of lives [2]. Therefore, efforts to reduce the flood probability through effective structural controls are important. Urban development results in a significant increase in impermeable surfaces that hinder the surface infiltration and increase the risk of floods [3]. Thus, innovative approaches, such as using permeable pavement surfaces, are becoming increasingly attractive.

A typical permeable pavement consists of a permeable upper surface, with a layer of 2 to 6 mm diameter bedding gravel, under which lies a base course layer, above natural soil (subgrade). The base course layer consists of aggregate, capable of providing both strength and the ability to store infiltrated water [4–7] (Figure 1). As incident rainfall and surface runoff water reach the pavement, it infiltrates through the pavers into the base course layer and may subsequently infiltrate to the subgrade soil, allowing for groundwater recharge [8–11]. This infiltration of stormwater reduces the volume and rate of runoff that would otherwise go through to the stormwater collection system [12]. This reduction in the peak volumetric flow of water is important in reducing the flooding probability in urban areas [8].

Previous studies indicate that permeable pavements can reduce the total surface runoff within a range of 1–40% and the peak flow by 7–43%, depending on the constructed system [10]. The Australian standard pavement design tool (DesignPave v2.0) [13] also supports these ranges of runoff reduction. Another study conducted in China found that more than 50% of road surface runoff can be reduced by using permeable pavements [14].

Other investigations have demonstrated that permeable pavements can perform well under extreme conditions [15–20], which makes them an environmentally attractive alternative to impermeable pavements, particularly in terms of flood control. Reducing the runoff water can eventually reduce the extent of drainage system requirements for stormwater collection [8,21,22] and, consequently, might reduce the carbon footprint of drainage construction. The reuse of water collected in the pavement can also reduce the energy/carbon footprint for reduced supply requirements of that water to households [23]. The use of permeable pavements, thus, complies with the sustainable development goals of the United Nations by ensuring the sustainability of cities, sustainable consumption of resources, and actions to reduce carbon footprint [24]. However, the extent of benefits/costs of using permeable pavements is subject to detailed analysis [25–27], which is beyond the scope of this research. This research focuses on the efficient in-situ runoff control with permeable pavements for reducing the stormwater flow in urban areas, which is a means of increasing the sustainability of the stormwater management system. Therefore, it is important to assess the pavement design requirements for reducing runoff in varying conditions.

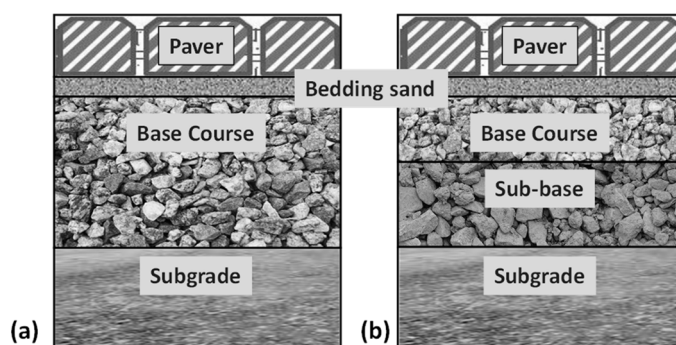


**Figure 1.** Typical permeable pavement configuration: (a) pavement containing only a granular base course, (b) pavement containing granular base and sub-base courses.

The required design thickness of a permeable pavement system designed to infiltrate water into its base course depends on several properties, such as surface infiltration rate, type of base course material, runoff volume resulting from the selected design rainfall intensity, the contributing area of the pavement, the subgrade infiltration rate and stormwater management objectives required for the pavement system [9,28]. Several previous studies have investigated both stormwater quantity and quality in permeable pavement systems [29–35], but there seems to be a distinct lack of information on the pavement base course thickness required to control peak stormwater flows, particularly in terms of how this varies spatially across Australia. Therefore, to assess the suitability of permeable pavements for reducing flood intensities in Australian conditions, this research spatially analysed the minimum base course thickness of permeable pavement systems across Australia for varying soil properties and rainfall data. Research conducted earlier for designing permeable pavements for urban catchments adopted the same methodology [36] as was implemented in this research. Previously research was also conducted to determine the design thickness of permeable pavements for parking lots aiming for runoff control [37]. However, a parametric study on the effects of rainfall and soil characteristics variability on the design thickness has not been previously analysed, which is one of the aims of this research.

The DesignPave v2.0 computer program [13] was used for the base course thickness assessments. DesignPave is the Australian standard permeable pavement design software. There are three types of permeable pavement in common use, namely porous concrete, permeable interlocking concrete paver (PICP), and porous asphalt [4]. This research focuses on the assessment of PICP only. PICP is particularly beneficial for the effective use of land, capable of supporting traffic movement on it immediately after construction, and can be designed for flood control, water harvesting and water quality improvement si-

multaneously [21,22]. The design life of PICP is also high compared to other types of permeable pavement and easy to operate and maintain [22], making it an effective solution for the desired water-sensitive urban design. This research is, therefore, useful because a spatial understanding of permeable pavement design thicknesses is important for planning purposes, particularly in the many Australian regions currently aspiring to promote the principles of efficient water use for a water-sensitive urban design.

## 2. Methods

### 2.1. Design Considerations

All pavements were designed for runoff control only, for a residential road design assuming full infiltration into the subgrade material, i.e., without embedded drainage pipes or impermeable linings. The DesignPave v2.0 modelling tool was used for all analyses. The surface of the pavement was assumed to be covered with a standard type of 80 mm thick pavers having openings along narrow joints (applicable for light traffic) [21], which has a permeability of  $9 \times 10^{-5}$  m/s. This paver thickness allows for vehicular traffic. Only uniform (single-sized diameter) granular material was assumed for the base course, which is recommended for residential applications [21] and it comes with very high permeability and water storage capacity due to its high void ratio. The permeability of subgrade soil, i.e., classification of subgrade soils, on the other hand, controls water infiltration, groundwater recharge and thus water storage in the base course, i.e., overall permeability in pavement design. Selecting other base course materials with lower void ratios would increase the design thickness, but that parametric analysis was not intended in this research. The pavement thickness was designed to accommodate additional runoff from nearby contributing areas. For this investigation, the design assessment was undertaken for a 100 m<sup>2</sup> permeable paving area with an additional 100 m<sup>2</sup> contributing area for residential development.

Australian Rainfall Runoff (ARR) 2016 Intensity–Frequency–Duration relationships [38] were used for the rainfall data and temporal patterns. The pavement system was designed based on an Annual Exceedance Probability (AEP) of 5% with a storm duration of 30 min (representing a moderate pattern of rainfall intensity). Pre-burst rainfall was not considered in the analysis. While the runoff coefficient can be up to 0.91 for built-up city areas, the design thickness was estimated considering an allowable runoff coefficient of 0.30, since permeable pavements significantly reduce the runoff rate [39]. A range of California Bearing Ratio (CBR), depending on the type of subgrade, was considered to evaluate the influence of subgrade soil classification on design base course thickness, e.g., 3–5% for clay, 10% for poorly graded sand and sand with fines, 20% for well-graded sand and gravel with fines, and 50% for gravel [40,41].

The subgrade hydraulic conductivity is defined as the ratio of distance travelled by the infiltrating water over a period of time and is generally measured in m/s or cm/s or m/day [42]. It depends on the soil classification, which generally includes clay, sand, silt and gravel. The primary classifications were further sub-classified according to their grading. The ranges of hydraulic conductivities for various soil classifications are provided in Table 1. The assumed design value in Table 1 is the mean value of these ranges and is often recommended for design when field hydraulic conductivity is unknown or not measured [13], and complements the typical values provided by Argue [43].

**Table 1.** Hydraulic conductivity of different soil types [13].

Soil Description	Hydraulic Conductivity Range (m/s)		Assumed Design Value (m/s)
	Min.	Max.	
Well-graded sands	$5 \times 10^{-6}$	$5 \times 10^{-4}$	$2.5 \times 10^{-4}$
Poorly graded sands and gravelly sands	$5 \times 10^{-7}$	$5 \times 10^{-6}$	$3 \times 10^{-6}$
Silty sands	$10^{-9}$	$5 \times 10^{-6}$	$2.5 \times 10^{-6}$
Clayey sand	$10^{-9}$	$10^{-6}$	$5 \times 10^{-7}$
Well-graded gravel	$10^{-5}$	$10^{-3}$	$5 \times 10^{-4}$
Poorly graded gravels and gravel-sand mixtures	$5 \times 10^{-5}$	$10^{-3}$	$5 \times 10^{-4}$
Silty gravels	$10^{-8}$	$10^{-4}$	$5 \times 10^{-5}$
Clayey gravels	$10^{-8}$	$10^{-6}$	$5 \times 10^{-7}$
Inorganic silts, very fine sands, clayey fine sands	$10^{-9}$	$10^{-7}$	$5 \times 10^{-8}$
Inorganic clays, gravelly clays, sandy clays	$10^{-9}$	$10^{-8}$	$5 \times 10^{-9}$
Inorganic silts, elastic silts	$10^{-10}$	$10^{-9}$	$5 \times 10^{-10}$
Inorganic clays of high plasticity	$10^{-11}$	$10^{-9}$	$5 \times 10^{-10}$

## 2.2. Selection of Towns and Cities for Spatial Analysis

For the spatial analysis, towns and cities were selected across Australia aiming to have a uniform distribution. Moreover, a selection criterion was set: countryside towns and cities having a minimum population of 50 and 500, respectively. With this criterion, a total of 107 towns and cities were selected, showing a uniform distribution, as shown in the Australian map in Figure 2a.

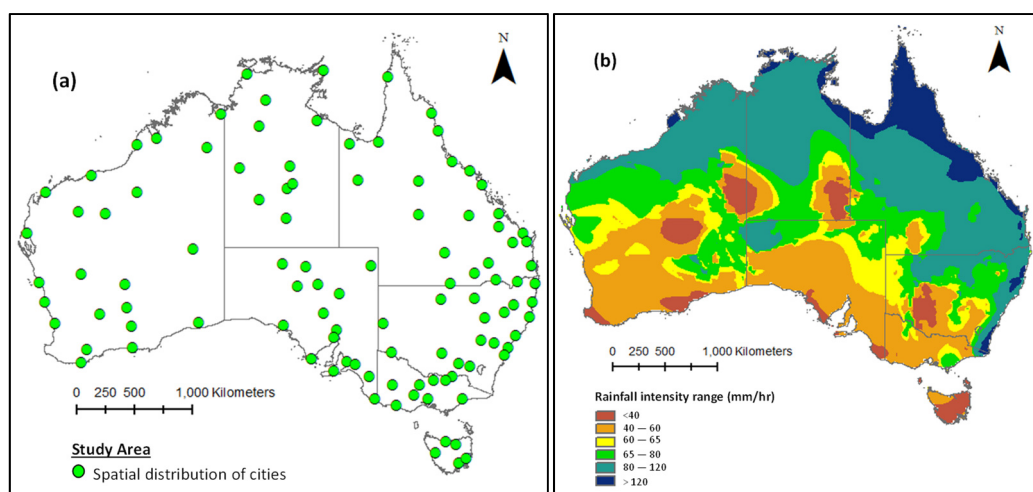


**Figure 2.** (a) Distribution of selected towns and cities for permeable pavement system assessment; (b) spatial distribution of rainfall intensity (mm/hour) (5% AEP, 30 min rainfall duration) across Australia based on the data for the selected towns and cities (data source: BOM [38]).

As mentioned earlier, many city councils in Australia consider an AEP of 5% with a storm duration of 30 min in their design. Thus, this study considered AEP of 5% and 30-min rainfall for all 107 towns and cities. These rainfall intensities at 107 locations can be sourced from ARR via the Bureau of Meteorology Design Rainfall Data System [38]. A spatial map of rainfall distribution across Australia, using the 5% AEP and 30-min rainfall duration rainfall intensity data (IFD) for these 107 locations is developed and presented in Figure 2b. The rainfall distribution map is an indication of the rainfall intensity considered

for this analysis for the selected cities. The spatial distribution was produced based on the 107 cities' data through a kriging interpolation method. Kriging is a Gaussian spatial interpolation method that estimates the value for unknown points based on the data of known points, and also considers the covariances of the known points while assessing for the unknown points [44,45]. Moreover, the kriging analysis output in this research was distributed following the raster dataset (cells representing any location) of the map. Therefore, it would not exactly match the actual rainfall distribution map. However, it complements the average annual rainfall distribution map of Australia [46].

### 2.3. Collection of Rainfall Data

Australia is sub-divided into twelve rainfall temporal zones [47], namely, Southern Slopes (Tasmania), Southern Slopes (mainland), Murray Basin, Central Slopes, East Coast South, East Coast North, Wet Tropics, Monsoonal North, Rangelands West, Rangelands, Flatlands West, and Flatlands East, which are aligned to assess the climate change impacts across Australia. The temporal distribution of rainfall (how rainfall falls over time) in these regions also varies depending on when 50% the heavy rainfall (burst) occurs, the burst categories (front/middle/back loaded) and the start and finish time of burst [47], along with some other factors. Figure 3 demonstrates the rainfall temporal regions along with their probable corresponding burst loading distributions. The burst loading indicates that the loading pattern of rainfall varies across the regions, some having a very high middle loading of rainfall while for some the middle loading peak is not much higher.

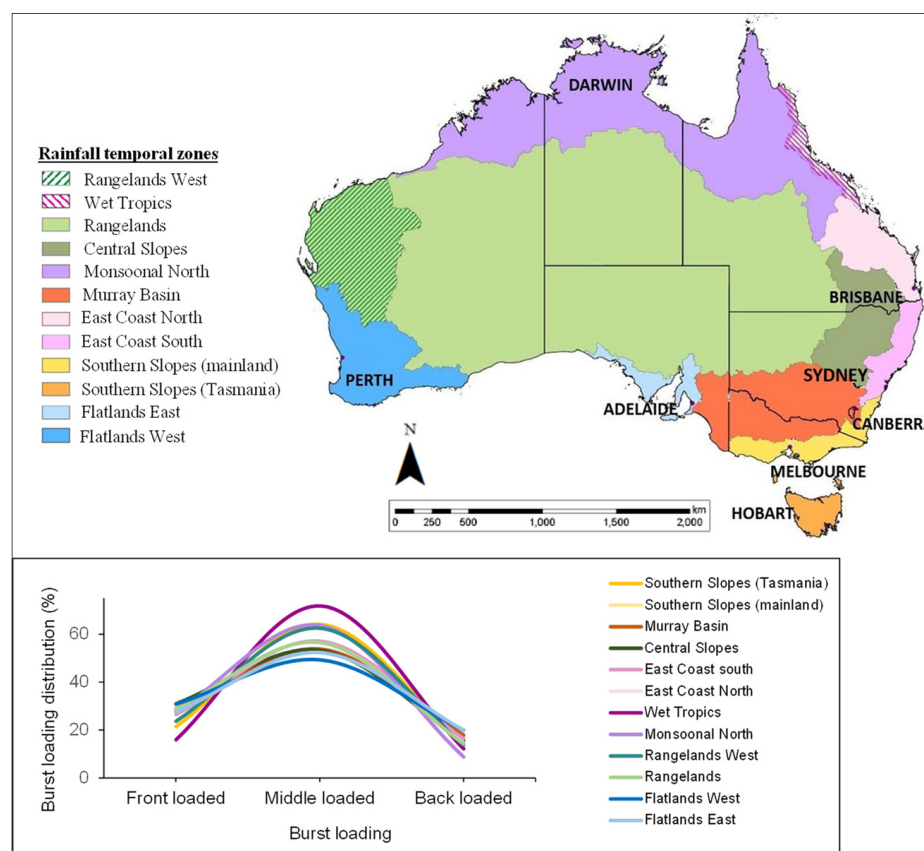


**Figure 3.** Rainfall temporal zone map of Australia indicating the front (FL), middle (ML) and back (BL) load distribution of rainfall bursts in the rainfall zones for <6 h of rainfall duration. Data adopted from Australian Rainfall and Runoff guideline [47].

The design rainfall (for flood control), therefore, would vary spatially for a known rainfall duration and AEP. As an example, the temporal distribution (in terms of the relative percentage) for four rainfall durations of 15, 30, 45 and 60 min at the 5-min

interval for Adelaide (southern Australia/Flatlands East region) and Darwin (northern Australia/Monsoonal North region) are shown in Figure 4a and 4b, respectively.

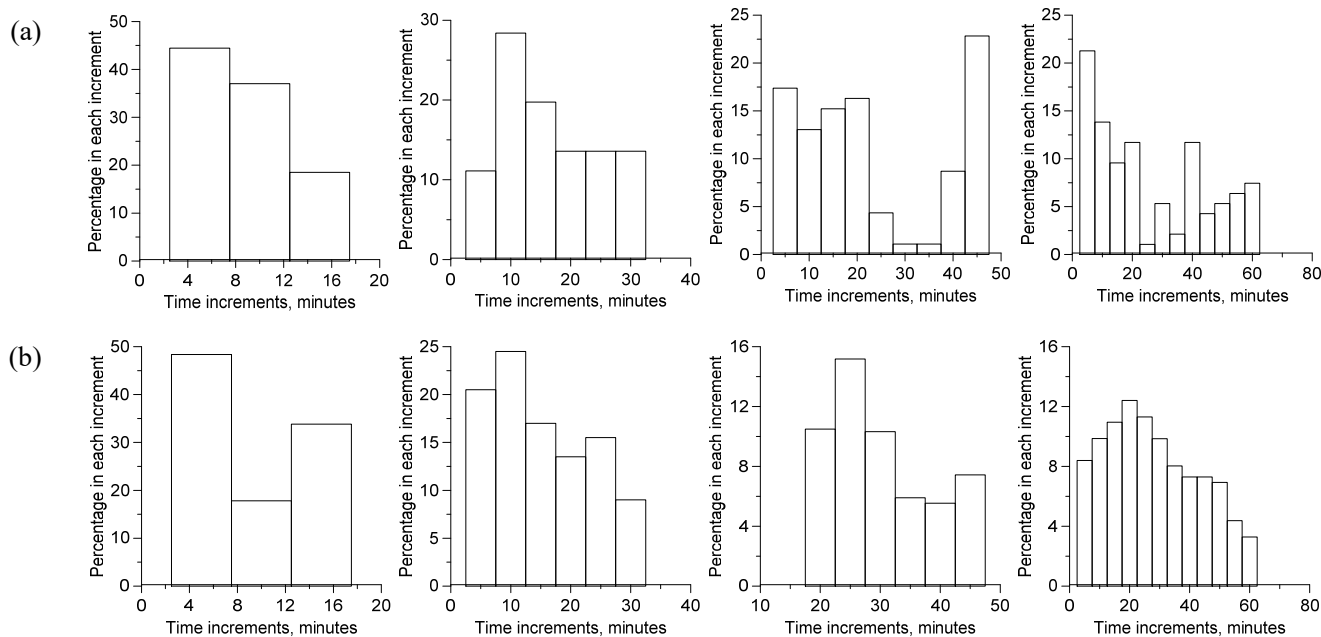


**Figure 4.** Example of rainfall temporal increment patterns for (a) Adelaide (southern Australia/Flatlands East region) and (b) Darwin (northern Australia/Monsoonal North region) for 4 rainfall durations (15, 30, 45, 60 min respectively from left to right). Data source: ARR [48].

Australian Rainfall and Runoff (ARR) is the national guideline for estimating design flood characteristics in Australia [48]. ARR provides the rainfall inputs, such as AEP rainfall intensity and its temporal distributions for rainfall duration of a zone, which significantly contribute to the formation of hydrograph, peak runoff and flood volume. Further, ARR provides a set of 10 probable temporal distributions, instead of one temporal distribution, for a known rainfall distribution and zone. For example, a set of 10 probable rainfall temporal distributions for 30-min rainfall for Adelaide and Darwin are shown in Figure 5a and 5b, respectively.

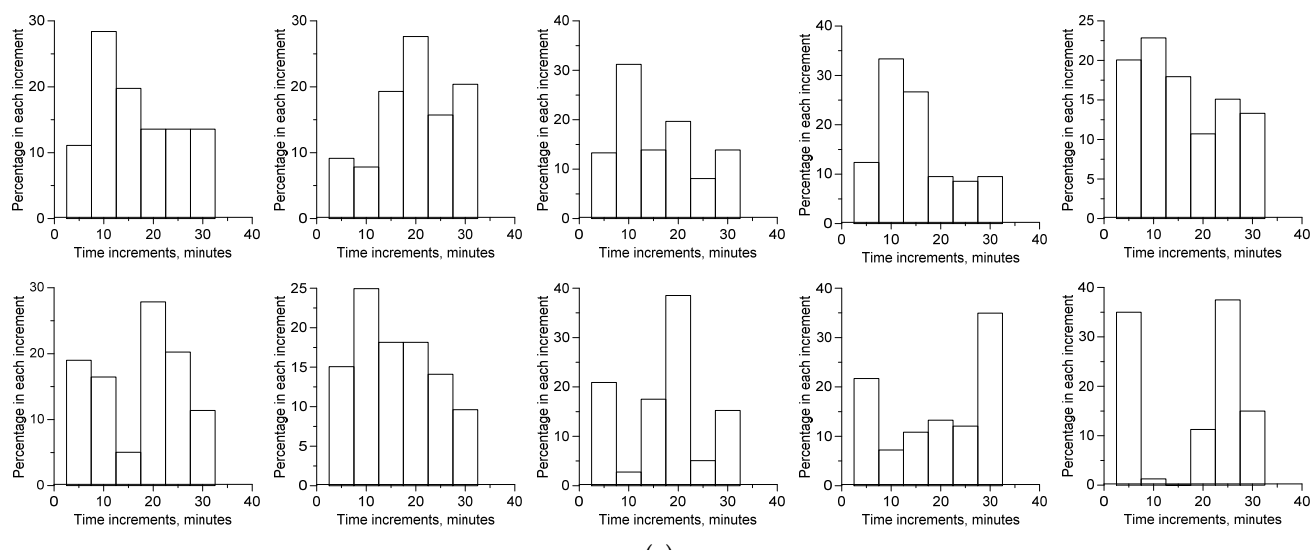
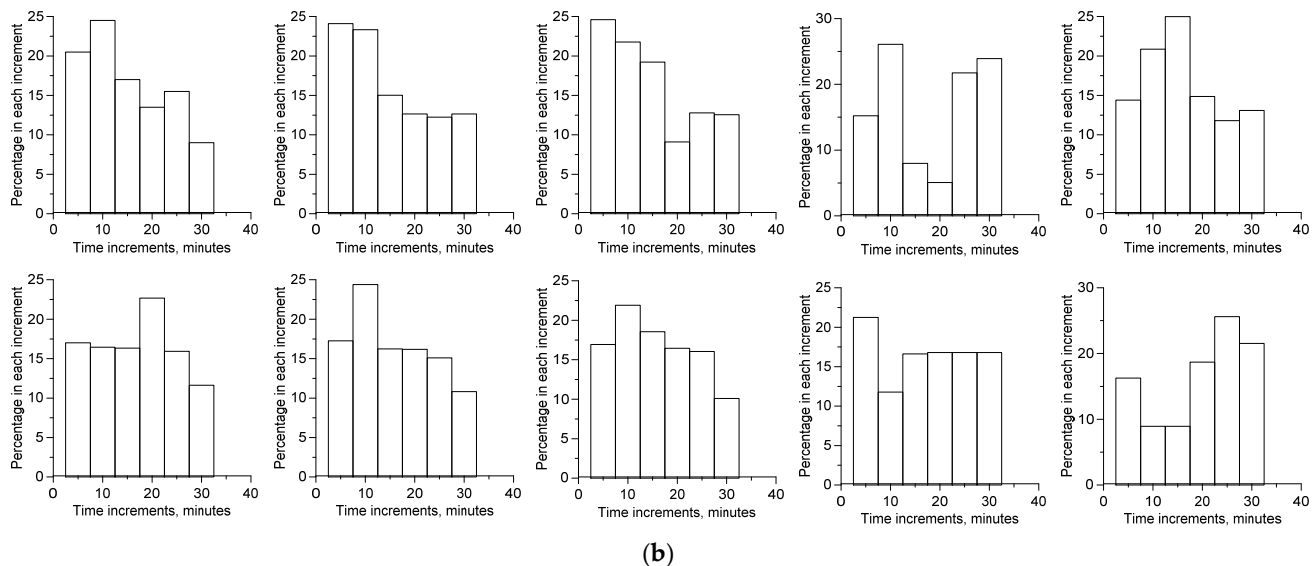


**Figure 5. Cont.**



(b)

**Figure 5.** Probable temporal distributions for a 30-min rainfall duration for (a) Adelaide (southern Australia/Flatlands East region) and (b) Darwin (northern Australia/Monsoonal North region), showing percentage distribution for each 5-min increment. Data source: ARR [48].

The corresponding 10 probable temporal distributions for all 107 towns and cities were considered to calculate hydrographs, which gives 10 different hydrographs for each location. For example, two sets of 10 different hydrographs for 10 probable rainfall temporal distributions for a duration of 30-min rainfall for Adelaide and Darwin are shown in Figure 6a and 6b, respectively. In this study, as representative rainfall distribution, the median of the ten peak inflow runoffs was considered for estimating the pavement design thicknesses for flood control and the corresponding hydrographs for Adelaide and Darwin are shown in Figure 6c and 6d, respectively.

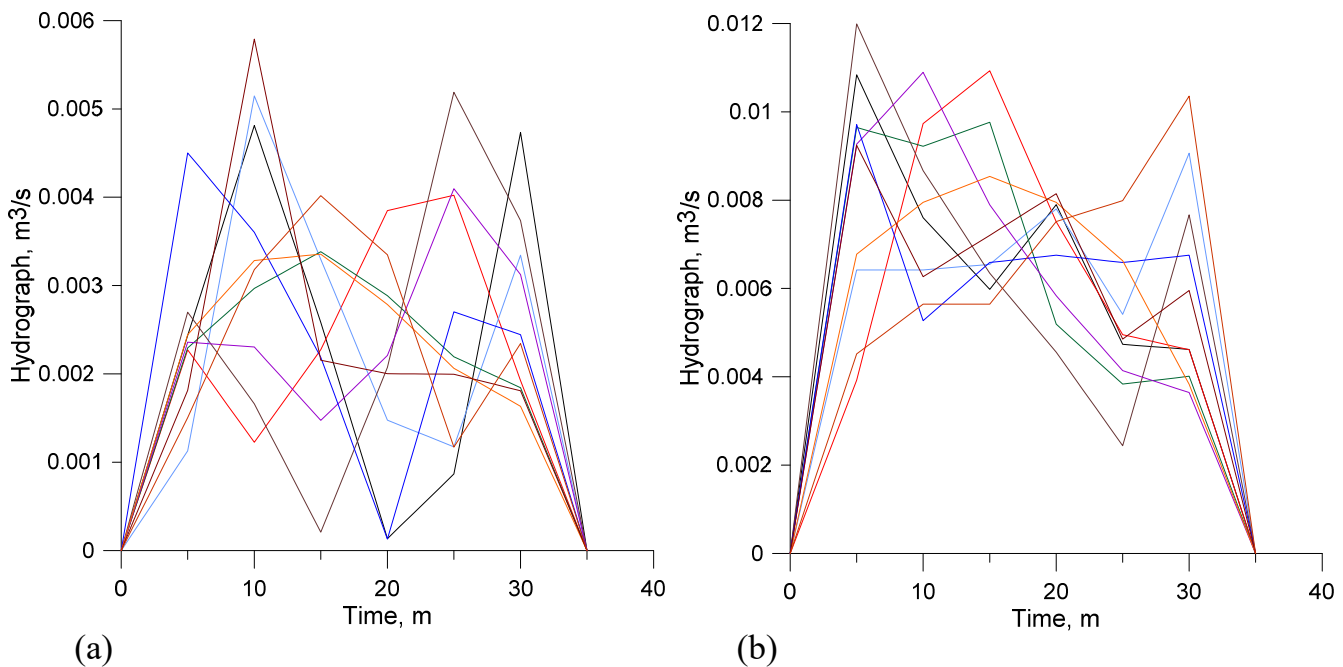


**Figure 6. Cont.**

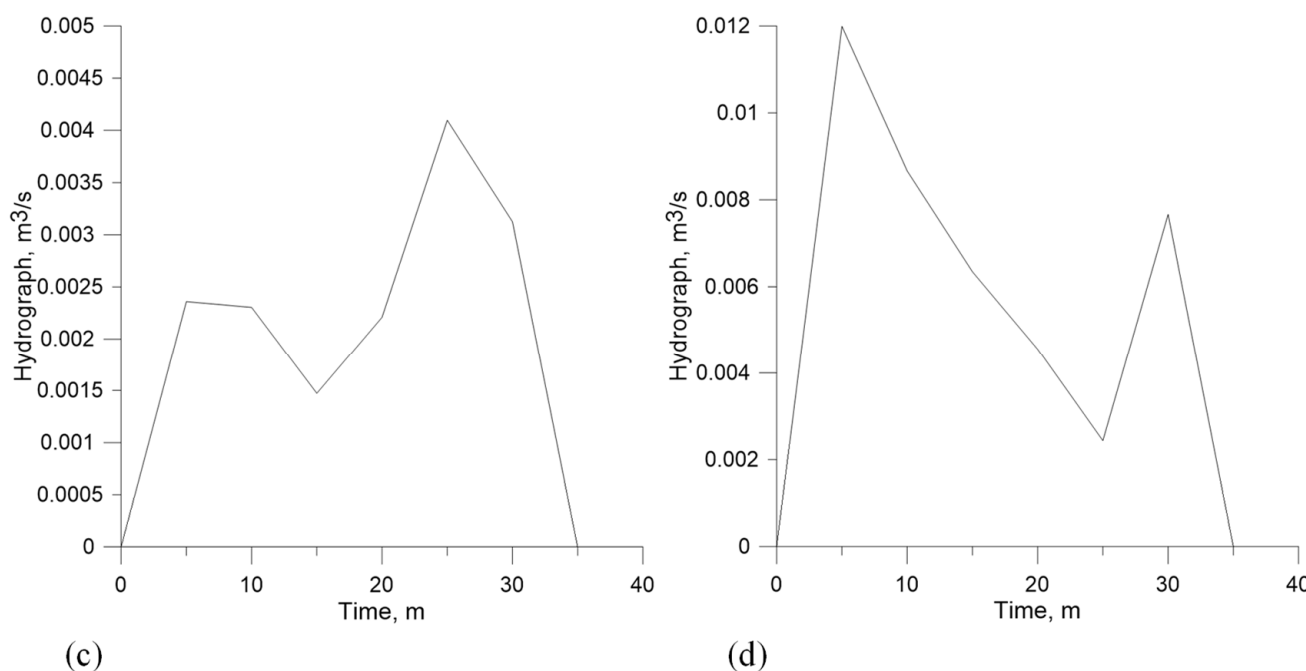


**Figure 6.** Probable runoff hydrographs for: (a) Adelaide (East Flatlands region); and (b) Darwin (Monsoonal North region) for a 30-min rainfall duration, with an Annual Exceedance Probability (AEP) of 5% on a  $200 \text{ m}^2$  catchment area. (c,d) shows the hydrographs of Adelaide and Darwin respectively for the median of peak inflow runoffs considered for design. Data source: ARR [48].

#### 2.4. Soil Types

The subgrade soil types for the selected towns and cities were determined using the Australian Government Soil Map [49] (Figure 7a), based on the Australian Soil Classification (ASC) system, which is classified based on the biological, chemical and physical properties of soils. The ASC is generally an agro-ecosystem classification that relates to soil health and particularly to its carbon and nutrient content, acidity, soil structure, topsoil thickness and salinity [49].

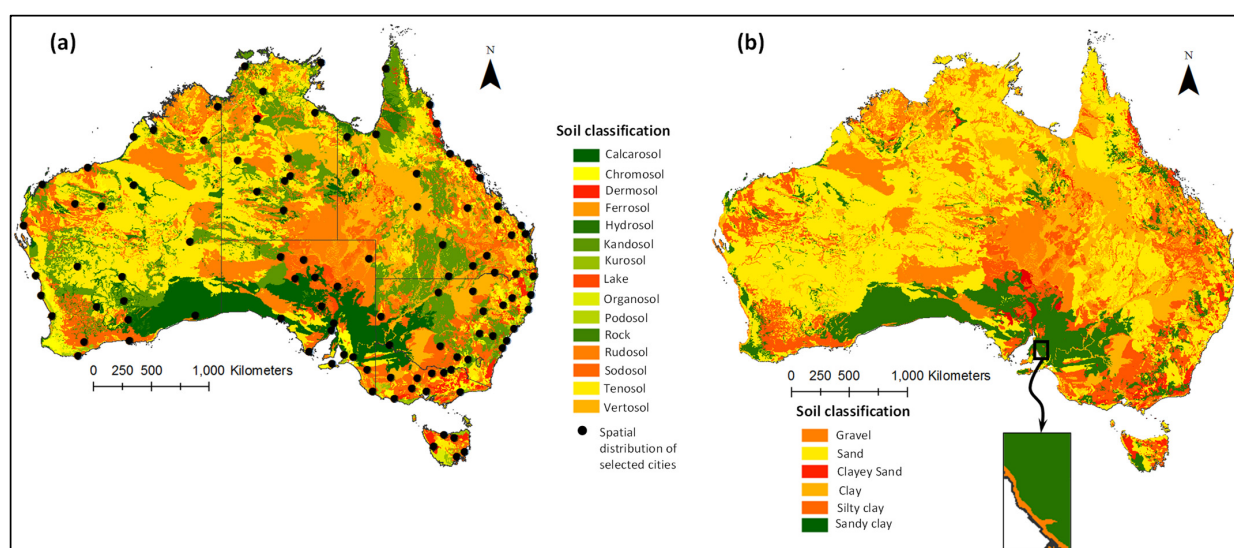


**Figure 7.** (a) ASC soil characteristics for selected towns and cities (Data source: SoE [49]; (b) interpreted geotechnical soil classification for the selected towns and cities (inset shows magnified soil classification for Adelaide, South Australia).

However, the agro-ecosystem soil classification, e.g., ASC (Figure 7a), and geotechnical classification as in Table 1 are not identical. Therefore, an algorithm was developed to derive the geotechnical soil classification (clay, sand, silt or gravel) from ASC, as shown in Figure 8. The interpretation algorithm was developed based on various assumptions, including matching the behaviour of the ASC and geotechnical soil classifications. The derived geotechnical classification did not consider the gradations and plasticity of soil for detailed subdivisions of the major classes. Therefore, the interpreted classification is considered as a tentative one and was used for further analysis in the absence of a detailed geotechnical soil classification map for Australia. Nevertheless, a statistical analysis was conducted in this study to assess the effect of soil gradations on the base course design thickness, which can offset this limitation.

As indicated in Table 1, sand and gravel soils are characterised by high subgrade hydraulic conductivity, meaning the infiltration rates would be high for these soils. Therefore, ferrosol, kandosol, kurosol, podosol and tenosol were classified as sands. Rudosol soil particles are very coarse and are formed from newly weathered rocks, so these were matched with gravel soil. Clay soil has very low permeability and depending on the soil mix, the clay soils were classified into clay, sandy clay or silty clay. Dermosol was considered as clayey sand, as it is sandy but has a significant clay content and thus has a lower hydraulic conductivity than sandy soil.

Considering the interpretation, the spatial distribution of the derived geotechnical soil classification map was prepared using ArcGIS (Figure 7b). The spatial map shows the dominance of sandy soils across Australia. The classification was considered suitable for further analysis as it matched with existing soil data. For example, Adelaide is characterised by clayey soil [50], and the interpreted classification also indicated sandy clay for Adelaide, with gravels along the coastline.

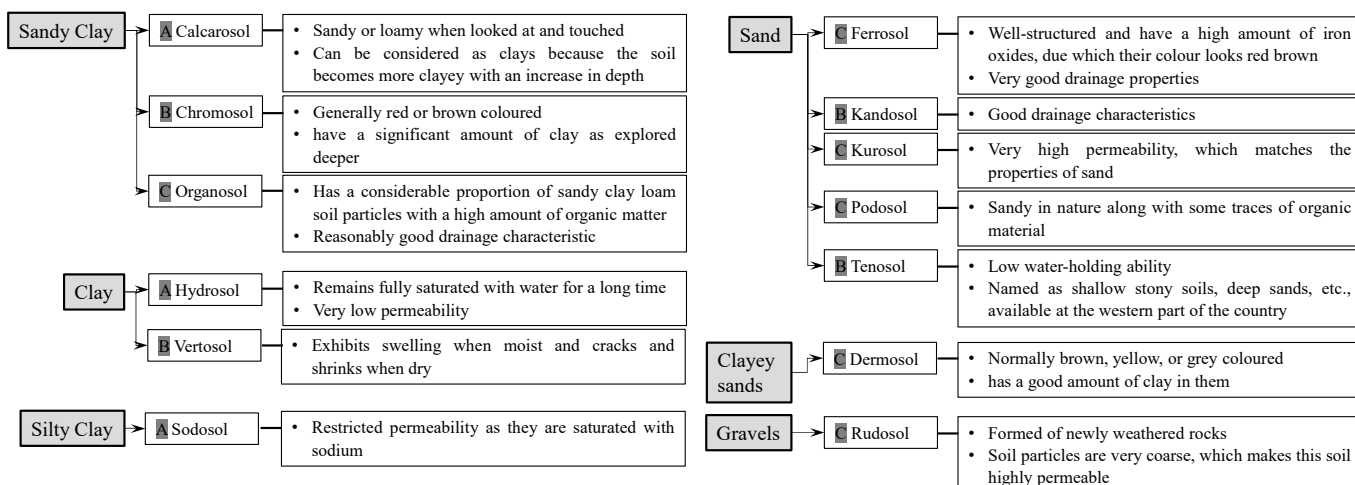


**Figure 8.** Interpretation of geotechnical soil classification from the Australian Soil Classification system (Data source: A: QLDGov [51]; B: GRDC [52]; C: VRO [53]).

## 2.5. Calculating Pavement Base Course Thickness: Hydraulic Design

The design thickness ( $D$ , mm) of the pavement base course depends on the rainfall rate, the pavement area ( $A$ ,  $\text{m}^2$ ) and the void ratio ( $VR$ , %) of the base course (Equation (1)).

$$D = \frac{(PI - HC) \times T}{A \times VR} \quad (1)$$

The pavement area and void ratio of the material depend on the design requirements. The amount of water that needs to be stored in the base course depends on the maximum paver inflow rate ( $PI$ ,  $\text{m}/\text{s}$ ) for the selected paver, the subgrade hydraulic conductivity ( $HC$ ,  $\text{m}/\text{s}$ ) for the relevant soil class, and the rainfall duration ( $T$ ).

The amount of water that infiltrates through the surface (L/s) is either the paver infiltration capacity irrespective of the rainfall received ( $PIC$ , L/s) or it is the rainfall rate received on the pavement ( $R$ , L/s), whichever is lower (Equation (2)).

$$PI = \min(PIC, R) \quad (2)$$

Therefore, the run-on or the amount of water spilled over the surface ( $PS$ , L/s) would be the difference between the rainfall rate ( $R$ , L/s) and the paver inflow capacity (Equation (3)).

$$PS = (R - PIC) \quad (3)$$

The total outflow ( $PO$ , L/s) from the pavement system would be the difference between the rainfall rate and the combination of the subgrade infiltration (function of  $HC$  and area) ( $SI$ , L/s) and the paver infiltration ( $PI$ , L/s) rate (Equation (4)).

$$PO = (R - (HC + PI)) \quad (4)$$

If the total outflow is more than the permissible discharge ( $PD$ , L/s) (which assumes a runoff coefficient of 0.3), the pavement design thickness is increased to increase storage of infiltrated water in the base course (Equation (5)).

$$\text{if } (PO > PD), D = D+, \text{ until } PO \leq PD \quad (5)$$

### 3. Results and Discussion

#### 3.1. Relations: Design Thickness vs. Permeability vs. Rainfall Intensity

The permeable pavement design parameters, soil classification and rainfall intensity for 107 towns and cities were considered for estimating the probable design thickness across Australia. This produced a relationship between the rainfall intensity and design thickness for different soil classifications (Figure 9). The design thickness generally needs to be higher if the rainfall intensity is higher or soil permeability is lower. For soils with high permeability, the effect of rainfall intensity is much less significant. Therefore, the estimated required design thickness is the minimum accepted value of 100 mm (to ensure the structural integrity for light-traffic load [54]) for gravel and sands with higher permeability (well-graded sand, permeability up to  $5 \times 10^{-4}$  m/s). For lower subgrade permeabilities, the design thickness follows a positive linear relationship with rainfall intensity.

The permeability of sandy soils is generally high. However, the proportion of fines, especially clay, is often found to determine the design thickness. This can be seen through a comparison of (non-clay) poorly graded sand and silty sand compared to clayey sand in Figure 10a. The poorly graded sand and silty sand have relatively higher permeability than clayey sand and, therefore, require a smaller design thickness but still follow the same increasing linear trend with rainfall.

When clay soils are dominant, the results suggest an insignificant difference in the design thicknesses (Figure 10b) for all sub-classes. Even the clayey sand has a similar level of permeability (Figure 9). The subgrade infiltration rate remains very low for all soil types (Figure 9), which results in a similar base course thickness to accommodate the surface runoff (Figure 10b). Soil with a gravel dominance generally has a very high subgrade infiltration rate. However, areas with clayey gravel require increased design thicknesses (this increases exponentially with rainfall intensity) than the minimum thickness required at well-graded gravel sites (Figure 10c).

Figure 10 indicates that up to a rainfall intensity of approximately 50 mm/h, a minimum base course thickness of 100–110 mm can serve for flood control purposes, whereas a base course thickness of 130 mm is required for a rainfall intensity up to 60 mm/h, irrespective of the soil classification. Above 60 mm/h, the design thickness tends to increase almost linearly. Thus, as a whole, a linear relationship is observed (Figure 10a,b) for the change in design thickness with rainfall intensity for the majority of soil classifications and gradations.

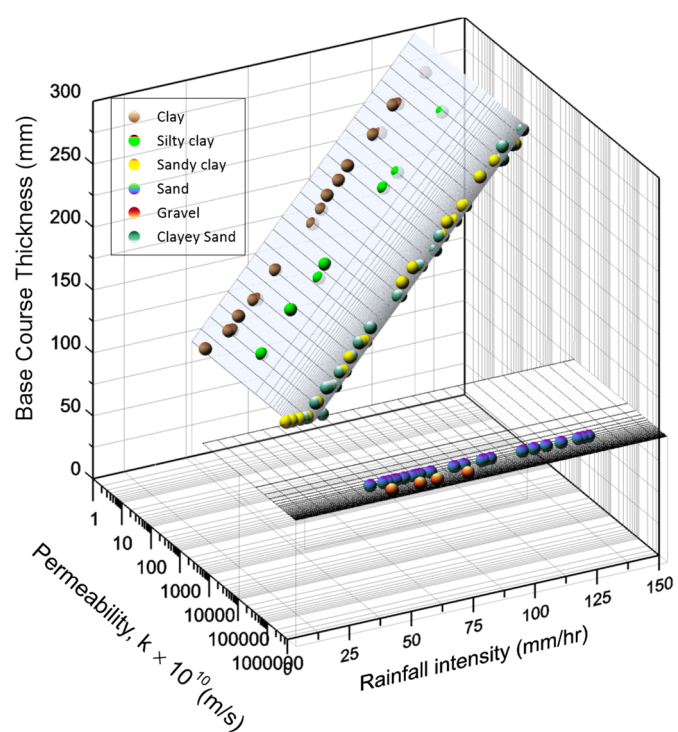


**Figure 9.** Base course thickness for variations in soil permeability and rainfall intensity.

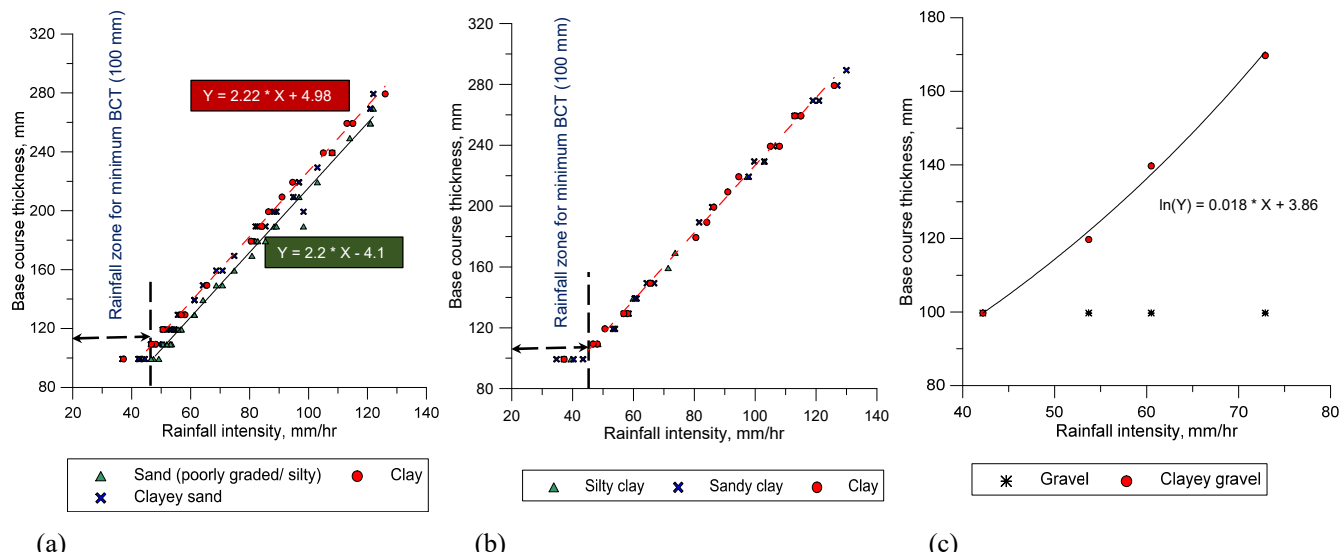


**Figure 10.** Relationship of base course thickness with rainfall intensity for various soil classifications: (a) thickness for different sand classifications and clay soils; (b) estimated thickness for different classes of clay soils; (c) estimated change in thickness for categories of gravel soils.

### 3.2. Spatial Distribution of Design Thickness

Based on the developed relationships between design thickness, rainfall intensity and soil class, the minimum base course design thicknesses for permeable pavements throughout Australia that enable full infiltration through the subgrade were estimated and the results are presented in Figure 11. The differences in hydraulic conductivity between the sand classes are the determining factors for design thicknesses. Therefore, two spatial analyses were conducted, one considering all sand and gravel soils as well graded (Figure 11a) and another considering all sand and gravel soils as poorly graded or silty sand (Figure 11b).

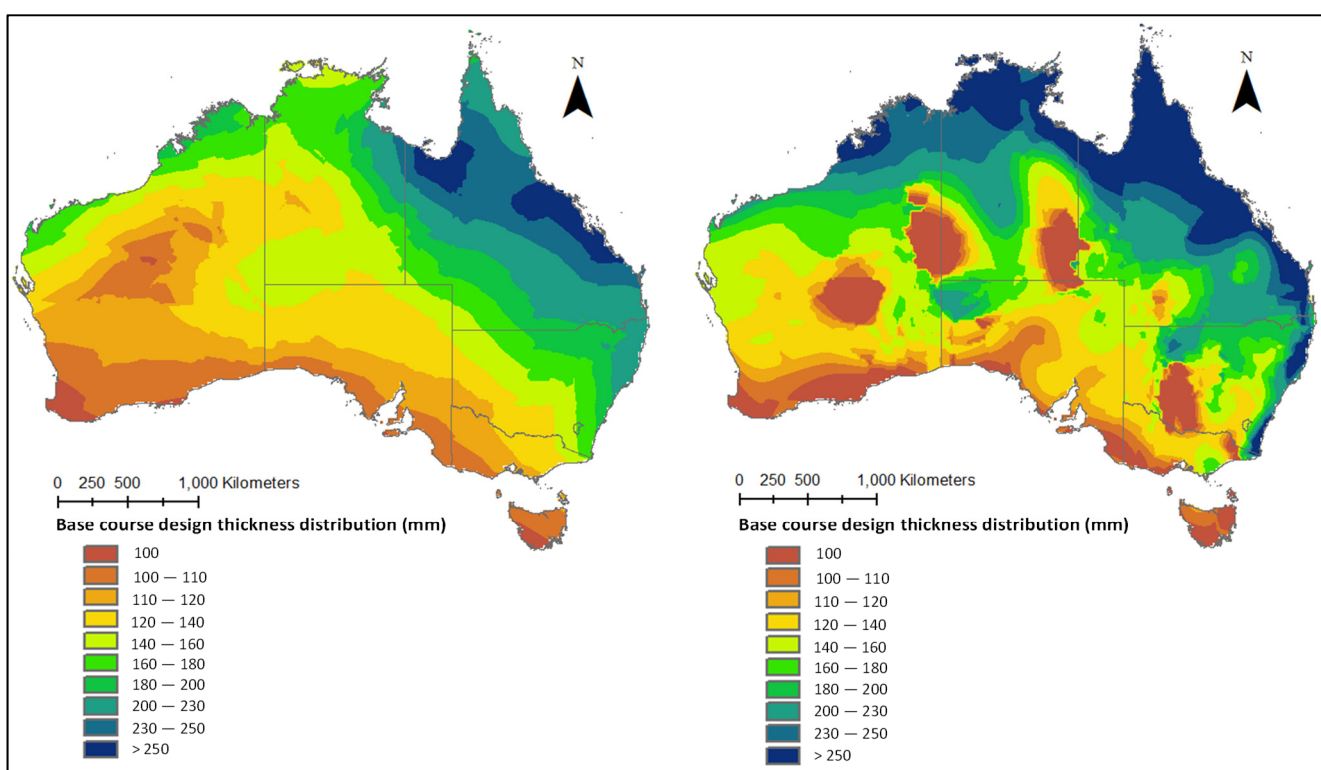


**Figure 11.** Estimated permeable pavement base course thickness distribution throughout Australia considering (a) well-graded sand and gravel soils, and (b) non-clay poorly graded sand and gravel soils.

Considering only well-graded sand throughout demonstrates a clear stratification of base course thickness requirements (Figure 11a). The kriging interpolation analysis considers the influence of known points to predict the spatial variability of unknown points. Thus, the generated probabilistic spatial map showed zonations in line with the soil classification zonations, as all the sandy soil sites required the minimum base course design thickness. The influence of rainfall created the zonations within silty or clayey soils. For example, although Adelaide, which is in the semi-arid southern zone of Australia, is characterised with clayey soils (Figure 7b), the lower rainfall intensities (Figure 2b) result in minimum base course thicknesses for this area.

When sandy soils are considered as poorly graded, the design thickness stratification becomes further segmented, due to the hydraulic conductivity and the base course vs. rainfall relationship generated in Figure 10a. However, in general, it is evident from Figure 11 that the pavement design thickness is lower in the southern, western and central parts of Australia. At least one-third of Australia requires a design thickness less than 120 mm, largely because of the common rainfall patterns. The high rainfall and clayey soils in the north-eastern zones result in the highest design thicknesses (more than 250 mm) for controlling surface runoff and urban flooding.

#### 4. Conclusions

This study has presented a spatial analysis of permeable pavement designs across the continent of Australia using the latest hydrological design procedures. It has demonstrated the strong influence of both subgrade soil type and rainfall intensity on design characteristics. Due to the predominance of sandy soils and low rainfall intensities in much of the west, south-west and central parts of Australia, a minimum base course design thickness of 100 mm is often sufficient. However, Australia also has high-rainfall tropical regions and areas with dense clay subgrades and so the spatial distributions of base course thickness, presented here, will be useful for planning purposes, particularly for regulatory

and consenting authorities that seek to promote the principles of water-sensitive urban design. The spatial distribution was analysed based on some assumptions (viz., sandy soil gradations, hydraulic conductivity of subgrade, void ratio of the materials). Still, the parametric analysis indicated the extent of design thickness variations for the variability of parameters.

**Author Contributions:** Conceptualization, A.I., M.M.R. and S.B.; Formal analysis, A.I. and M.M.R.; Methodology, A.I., M.M.R. and S.B.; Validation, S.B.; Visualization, A.I.; Writing—original draft, A.I.; Writing—review & editing, M.M.R. and S.B. All authors have read and agreed to the published version of the manuscript.

**Funding:** This research received no external funding.

**Data Availability Statement:** Not applicable.

**Acknowledgments:** The authors acknowledge the support and collaboration of Concrete Masonry Association of Australia in the development of DesignPave v2.0 software.

**Conflicts of Interest:** The authors declare no conflict of interest.

## References

1. Ladds, M.; Keating, A.; Handmer, J.; Magee, L. How much do disasters cost? A comparison of disaster cost estimates in Australia. *Int. J. Disaster Risk Reduct.* **2017**, *21*, 419–429. [[CrossRef](#)]
2. Nafari, R.H.; Ngo, T.; Mendis, P. An Assessment of the Effectiveness of Tree-Based Models for Multi-Variate Flood Damage Assessment in Australia. *Water* **2016**, *8*, 282. [[CrossRef](#)]
3. Yamashita, S.; Watanabe, R.; Shimatani, Y. Smart adaptation to flooding in urban areas. *Procedia Eng.* **2015**, *118*, 1096–1103. [[CrossRef](#)]
4. Razzaghmanesh, M.; Beecham, S. A Review of Permeable Pavement Clogging Investigations and Recommended Maintenance Regimes. *Water* **2018**, *10*, 337. [[CrossRef](#)]
5. Drake, J.A.; Bradford, A.; Marsalek, J. Review of environmental performance of permeable pavement systems: State of the knowledge. *Water Qual. Res. J. Can.* **2013**, *48*, 203–222. [[CrossRef](#)]
6. Saadeh, S.; Ralla, A.; Al-Zubi, Y.; Wu, R.; Harvey, J. Application of fully permeable pavements as a sustainable approach for mitigation of stormwater runoff. *Int. J. Transp. Sci. Technol.* **2019**, *8*, 338–350. [[CrossRef](#)]
7. Dai, K.; Liu, W.; Shui, X.; Fu, D.; Zevenbergen, C.; Singh, R.P. Hydrological Effects of Prefabricated Permeable Pavements on Parking Lots. *Water* **2022**, *14*, 45. [[CrossRef](#)]
8. Imran, H.M.; Akib, S.; Karim, M.R. Permeable pavement and stormwater management systems: A review. *Environ. Technol.* **2013**, *34*, 2649–2656. [[CrossRef](#)]
9. Kamali, M.; Delkash, M.; Tajrishy, M. Evaluation of permeable pavement responses to urban surface runoff. *J. Environ. Manag.* **2017**, *187*, 43–53. [[CrossRef](#)]
10. Hu, M.; Zhang, X.; Siu, Y.L.; Li, Y.; Tanaka, K.; Yang, H.; Xu, Y. Flood Mitigation by Permeable Pavements in Chinese Sponge City Construction. *Water* **2018**, *10*, 172. [[CrossRef](#)]
11. Alyaseri, I.; Zhou, J. Stormwater Volume Reduction in Combined Sewer Using Permeable Pavement: City of St. Louis. *J. Environ. Eng.* **2016**, *142*, 04016002. [[CrossRef](#)]
12. Andres-Valeri, V.C.; Juli-Gandara, L.; Jato-Espino, D.; Rodriguez-Hernandez, J. Characterization of the Infiltration Capacity of Porous Concrete Pavements with Low Constant Head Permeability Tests. *Water* **2018**, *10*, 480. [[CrossRef](#)]
13. CMAA. DesignPave Software. Available online: <https://www.cmaa.com.au/DesignPave/faq> (accessed on 8 June 2020).
14. Zhu, H.; Yu, M.; Zhu, J.; Lu, H.; Cao, R. Simulation study on effect of permeable pavement on reducing flood risk of urban runoff. *Int. J. Transp. Sci. Technol.* **2019**, *8*, 373–382. [[CrossRef](#)]
15. Liu, W.; Feng, Q.; Chen, W.; Deo, R.C. Stormwater runoff and pollution retention performances of permeable pavements and the effects of structural factors. *Environ. Sci. Pollut. Res.* **2020**, *27*, 30831–30843. [[CrossRef](#)] [[PubMed](#)]
16. Li, H.; Harvey, J.T.; Holland, T.J.; Kayhanian, M. The use of reflective and permeable pavements as a potential practice for heat island mitigation and stormwater management. *Environ. Res. Lett.* **2013**, *8*, 015023. [[CrossRef](#)]
17. Liu, Q.; Liu, S.; Hu, G.; Yang, T.; Du, C.; Oeser, M. Infiltration capacity and structural analysis of permeable pavements for sustainable urban: A full-scale case study. *J. Clean. Prod.* **2021**, *288*, 125111. [[CrossRef](#)]
18. Lin, W.; Kim, I.T.; Kim, H.; Cho, Y.-H. Water Runoff Characteristics in Porous Block Pavements Using an Accelerated Pavement Tester. *J. Hydrol. Eng.* **2014**, *19*, 04014012. [[CrossRef](#)]
19. Kia, A.; Delens, J.M.; Wong, H.S.; Cheeseman, C.R. Structural and hydrological design of permeable concrete pavements. *Case Stud. Constr. Mater.* **2021**, *15*, e00564. [[CrossRef](#)]
20. Yang, Q.; Dai, F.; Beecham, S. The influence of evaporation from porous concrete on air temperature and humidity. *J. Environ. Manag.* **2022**, *306*, 114472. [[CrossRef](#)]

21. CMAA. *PE01- Permeable Interlocking Concrete Pavements Design and Construction Guide*; Concrete Masonry Association of Australia (CMAA): Sydney, Australia, 2010.
22. Smith, D.R. *Permeable Interlocking Concrete Pavement [Techbrief]*; Federal Highway Administration: Washington, DC, USA, 2019.
23. Antunes, L.N.; Sydney, C.; Ghisi, E.; Phoenix, V.R.; Thives, L.P.; White, C.; Garcia, E.S.H. Reduction of Environmental Impacts Due to Using Permeable Pavements to Harvest Stormwater. *Water* **2020**, *12*, 2840. [[CrossRef](#)]
24. SDGS. Sustainable Development Goals. Available online: <https://sdgs.un.org/goals> (accessed on 25 March 2022).
25. Singh, A.; Vaddy, P.; Biligiri, K.P. Quantification of embodied energy and carbon footprint of pervious concrete pavements through a methodical lifecycle assessment framework. *Resour. Conserv. Recycl.* **2020**, *161*, 104953. [[CrossRef](#)]
26. Rahman, M.M.; Beecham, S.; Iqbal, A.; Karim, M.R.; Rabbi, A.T.Z. Sustainability Assessment of Using Recycled Aggregates in Concrete Block Pavements. *Sustainability* **2020**, *12*, 4313. [[CrossRef](#)]
27. Rahman, M.M.; Hora, R.N.; Ahenkorah, I.; Beecham, S.; Karim, M.R.; Iqbal, A. State-of-the-Art Review of Microbial-Induced Calcite Precipitation and its Sustainability in Engineering Applications. *Sustainability* **2020**, *12*, 6281. [[CrossRef](#)]
28. Yang, Q.; Beecham, S.; Liu, J.; Pezzaniti, D. The influence of rainfall intensity and duration on sediment pathways and subsequent clogging in permeable pavements. *J. Environ. Manag.* **2019**, *246*, 730–736. [[CrossRef](#)] [[PubMed](#)]
29. Liu, J.; Yan, H.; Liao, Z.; Zhang, K.; Schmidt, A.R.; Tao, T. Laboratory analysis on the surface runoff pollution reduction performance of permeable pavements. *Sci. Total Environ.* **2019**, *691*, 1–8. [[CrossRef](#)]
30. Disfani, M.M.; Mohammadinia, A.; Narsilio, G.A.; Aye, L. Performance evaluation of semi-flexible permeable pavements under cyclic loads. *Int. J. Pavement Eng.* **2020**, *21*, 336–346. [[CrossRef](#)]
31. Braswell, A.S.; Winston, R.J.; Hunt, W.F. Hydrologic and water quality performance of permeable pavement with internal water storage over a clay soil in Durham, North Carolina. *J. Environ. Manag.* **2018**, *224*, 277–287. [[CrossRef](#)]
32. Selbig, W.R.; Buer, N.; Danz, M.E. Stormwater-quality performance of lined permeable pavement systems. *J. Environ. Manag.* **2019**, *251*, 109510. [[CrossRef](#)]
33. Chu, L.; Fwa, T.F. Evaluation of surface infiltration performance of permeable pavements. *J. Environ. Manag.* **2019**, *238*, 136–143. [[CrossRef](#)]
34. Xie, J.; Jia, S.; Li, H.; Gao, L. Study on the influence of clogging on the cooling performance of permeable pavement. *Water* **2018**, *10*, 299. [[CrossRef](#)]
35. Alsubih, M.; Arthur, S.; Wright, G.; Allen, D. Experimental study on the hydrological performance of a permeable pavement. *Urban Water J.* **2017**, *14*, 427–434. [[CrossRef](#)]
36. Hong, Y.-M. The simplified design method of permeable pavement system for urban catchment. *Environ. Chall.* **2021**, *2*, 100014. [[CrossRef](#)]
37. Rushton, B.T. Low-Impact Parking Lot Design Reduces Runoff and Pollutant Loads. *J. Water Resour. Plan. Manag.* **2001**, *127*, 172–179. [[CrossRef](#)]
38. BOM. Design Rainfall Data System. Available online: <http://www.bom.gov.au/water/designRainfalls/revised-ifd/> (accessed on 12 December 2021).
39. Coombes, P.; Roso, S. (Eds.) *Runoff in Urban Areas, Book 9 in Australian Rainfall and Runoff—A Guide to Flood Estimation*; Geoscience Australia: Barton, ACT, Australia, 2019.
40. Wilches, F.J.; Burbano, J.L.A.; Sierra, E.E.C. Subgrade soils characterization data, for correlation of geotechnical variables on urban roads in northern Colombia. *Data Brief* **2020**, *32*, 106095. [[CrossRef](#)] [[PubMed](#)]
41. Gilson. California Bearing Ratio Test: CBR Values & Why They Matter. Available online: <https://www.globalgilson.com/blog/cbr-testing> (accessed on 22 January 2022).
42. Chung, C.-K.; Kim, J.-H.; Kim, J.; Kim, T. Hydraulic Conductivity Variation of Coarse-Fine Soil Mixture upon Mixing Ratio. *Adv. Civ. Eng.* **2018**, *2018*, 6846584. [[CrossRef](#)]
43. Argue, J.R. (Ed.) *Water Sensitive Urban Design: Basic Procedures for ‘Source Control’ of Stormwater*; University of South Australia: Adelaide, Australia, 2013.
44. Sharma, V.; Sharma, M.; Pandita, S.; Kour, J.; Sharma, N. 11-Application of geographic information system and remote sensing in heavy metal assessment. In *Heavy Metals in the Environment*; Kumar, V., Sharma, A., Cerdà, A., Eds.; Elsevier: Amsterdam, The Netherlands, 2021; pp. 191–204. [[CrossRef](#)]
45. Paramasivam, C.R.; Venkatramanan, S. Chapter 3-An Introduction to Various Spatial Analysis Techniques. In *GIS and Geostatistical Techniques for Groundwater Science*; Venkatramanan, S., Prasanna, M.V., Chung, S.Y., Eds.; Elsevier: Amsterdam, The Netherlands, 2019; pp. 23–30. [[CrossRef](#)]
46. BOM. Rainfall Percentiles. Available online: [http://www.bom.gov.au/jsp/ncc/climate\\_averages/rainfall-percentiles/index.jsp?maptype=12&period=Annual&product=50th#maps](http://www.bom.gov.au/jsp/ncc/climate_averages/rainfall-percentiles/index.jsp?maptype=12&period=Annual&product=50th#maps) (accessed on 12 January 2022).
47. Ball, J.; Babister, M.; Nathan, R.; Weeks, W.; Weinmann, E.; Retallick, M.; Testoni, I. (Eds.) *Australian Rainfall and Runoff: A Guide to Flood Estimation*; Geoscience Australia: Barton, ACT, Australia, 2019.
48. ARR. Australian Rainfall & Runoff: Data Hub. Available online: <http://data.arr-software.org/> (accessed on 12 December 2021).
49. SoE. 2016 SoE Land Australian Soil Classification Orders. Available online: <https://data.gov.au/dataset/ds-dga-116eb634-fc0b-42d8-ae27-b876a12c4f6a/details> (accessed on 25 February 2021).
50. DEW. Soils (Soil Type). Available online: <https://data.sa.gov.au/data/dataset/ae914203-50c3-4194-acc5-402c2cd62841> (accessed on 11 February 2022).

51. QLDGov. Common Soil Types. Available online: <https://www.qld.gov.au/environment/land/management/soil/soil-testing/types#:~{}:text=Calcarosols,rocks%2C%20limestone%20and%20windborne%20deposits> (accessed on 19 August 2021).
52. GRDC. Soils What Are We Talking About? Available online: <https://grdc.com.au/resources-and-publications/groundcover/ground-cover-issue-40-sa/soils-what-are-we-talking-about> (accessed on 19 August 2021).
53. VRO. Contenders for State Soil. Available online: [http://vro.agriculture.vic.gov.au/dpi/vro/vrosite.nsf/pages/soil\\_vic\\_contenders](http://vro.agriculture.vic.gov.au/dpi/vro/vrosite.nsf/pages/soil_vic_contenders) (accessed on 19 August 2021).
54. MCC. *Manual of Engineering Standards: 5- Pavement Design*; Maitland City Council: Maitland, NSW, Australia, 2018.